

Accepted Manuscript

Title: MWW layered zeolites modified with niobium species - surface and catalytic properties

Authors: Anna Wojtaszek-Gurdak, Martyna Zielinska, Maria Ziolk



PII: S0920-5861(18)31109-X
DOI: <https://doi.org/10.1016/j.cattod.2018.07.044>
Reference: CATTOD 11589

To appear in: *Catalysis Today*

Received date: 17-3-2018
Revised date: 23-5-2018
Accepted date: 15-7-2018

Please cite this article as: Wojtaszek-Gurdak A, Zielinska M, Ziolk M, MWW layered zeolites modified with niobium species - surface and catalytic properties, *Catalysis Today* (2018), <https://doi.org/10.1016/j.cattod.2018.07.044>

This is a PDF file of an unedited manuscript that has been accepted for publication. As a service to our customers we are providing this early version of the manuscript. The manuscript will undergo copyediting, typesetting, and review of the resulting proof before it is published in its final form. Please note that during the production process errors may be discovered which could affect the content, and all legal disclaimers that apply to the journal pertain.

MWW layered zeolites modified with niobium species - surface and catalytic properties

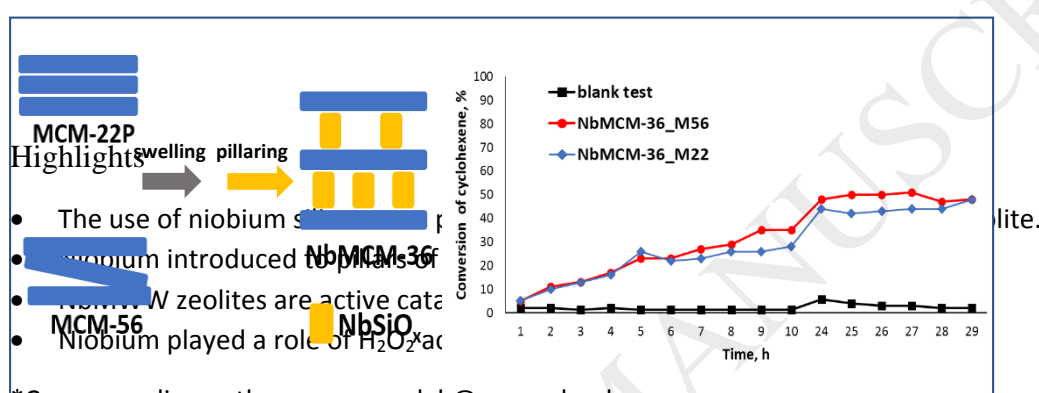
Anna Wojtaszek-Gurdak*, Martyna Zielinska, Maria Ziolk

Adam Mickiewicz University in Poznan, Faculty of Chemistry, Umultowska 89b, 61-614

Poznan, Poland

Graphical abstract

CYCLOHEXENE OXIDATION WITH H_2O_2



Abstract

New heterogeneous catalysts were obtained by modification of MWW zeolites (MCM-22 and MCM-56) by swelling and pillaring with niobiosilicate, achieved by two different methods. The main differences between these methods were time and temperature at which the modification was carried out, the concentration of a base used during the modification, and the water content in the catalysts used for further modification. The XRD analysis proved that both methods used gave MCM-36 structure, in all cases pillaring led to an increase in surface area, but some differences in final materials were noted, depending on the pillaring procedure. Both NbMCM-36 zeolites exhibited different content of micropores (lower in the zeolites synthesized from MCM-22), different loading with niobium species (higher in the material prepared from MCM-56) and similar acidity strength. Both niobium containing zeolites were active catalysts in liquid phase cyclohexene oxidation with H_2O_2 and were successfully used in the second run. Niobium

played a role of H₂O₂ activator. Texture parameters and content of niobium was crucial for the effective discoloration of methylene blue with the use of hydrogen peroxide.

Keywords: *MWW zeolites; NbMCM-36; cyclohexene oxidation; discoloration of methylene blue*

1. Introduction

Modification of zeolites by niobium species can be performed by isomorphous substitution during the synthesis or by post-synthesis modification. The first route is difficult if low silica zeolites are used (e.g. FAU type) and requires several steps [1,2], whereas it is easier for high silica zeolites (e.g. ZSM-5) prepared with the use of a template [3]. In the 21st century, different methods for niobium introduction have been developed because of attractive properties of zeolitic materials containing niobium, zeolites beta (BEA) became of interest. Dzwigaj et al. [4] have used the two-step post-synthesis method, at first dealumination process of BEA was performed to obtain vacant T sites associated with silanol groups and then the niobium ions were introduced into vacant T sites by impregnation with Nb(OC₂H₅)₅ as a metal precursor. So localized niobium species were components of the zeolite structure. In contrast, Corma et al. [5] have applied the direct introduction of Nb(V)ethoxide during BEA synthesis in fluoride media. They have obtained the zeolites with Si/Nb = 53 and 109. The location of niobium in BEA structure depended on the loading of the metal. The high loading of niobium (>1.5 wt%) introduced by Dzwigaj's method gave rise to the zeolites with a mixture of the framework mononuclear and extra-framework polynuclear Nb(V). Ab initio periodic DFT calculations [6, 7] indicated that niobium(V) was stabilized in the BEA framework at the penta-coordinated site with one hydroxyl group. The structure with Nb(V)O-H group and Nb linked by four Nb-OSi bonds to the zeolitic walls appeared as the most favorable.

Post synthesis modification with niobium source can also result in partial incorporation of niobium into zeolite framework. Such behavior was observed in modification of hydrogen

forms of layered MCM-22 and disordered MCM-56 zeolites [8]. However, generally, simple impregnation of zeolites with niobium source gives rise to the location of niobium species in the extra framework positions. The impregnation method used for the modification of TS-1 (titano-silicalite-1 zeolite of MFI structure) with niobium [9] resulted in octahedral coordination of niobium in Nb/TS-1 identified by UV-vis study which indicated that niobium oxide was localized in the extra framework positions. Recently, the hierarchical niobium-containing zeolites were synthesized and applied for isomerization of dihydroxyacetone to alkyl lactate and lactic acid [10]. These materials possess secondary mesoporosity, thus facilitating access to active sites of the material by larger reagent molecules, preserving acidity and crystallinity of the zeolites.

In this work, we focused on obtaining new heterogeneous catalysts by modification of MWW zeolites (MCM-22 and MCM-56) by swelling and pillaring with niobiosilicate. In this way, a new type of MCM-36 zeolite was formed. This type of modification should lead to three main effects: 1) the crystalline zeolitic layers together with the amorphous structure resulting from irregular arrangement of pillars should endow catalysts with dual nature, 2) the pillared zeolites will have dual porosity, microporous channels in the zeolitic layers and flat-shaped mesopores between the layers, 3) new type of active centers should be generated by Nb located in pillars. Two different methods of swelling and pillaring of MWW zeolites were used. One of them, used for the modification of MCM-22, was based on the Roth's procedure [11], whereas in the disordered MCM-56 zeolite, the Zhang's procedure [12] was applied for pillaring. The textural and structural properties of the materials obtained were characterized by N₂ adsorption/desorption and XRD measurements. The states of materials components were characterized by UV-vis and XPS spectroscopies, whereas the acidity of the surfaces was evaluated by test reaction and pyridine adsorption combined with FTIR measurements. The obtained niobium containing pillared zeolites were used as catalysts in two reactions in which

hydrogen peroxide was the oxidation agent, oxidation of cyclohexene and methylene blue discoloration.

2. Experimental

2.1. Synthesis of layered MWW zeolites

The MCM-22 and MCM-56 zeolites were synthesized using the same reagents: SiO₂ (Ultrasil 3VN – Degussa), sodium aluminate (53% of Al₂O₃ and 42.5% of Na₂O, Riedel-de Haen), distilled water, sodium hydroxide (Chempur), and hexamethyleneimine (HMI – Aldrich) as the template.

The MCM-22 zeolite was prepared according to the procedure described in Ref. [13] The synthesis gel had the following composition: SiO₂/Al₂O₃ = 54, OH/SiO₂ = 0.18, H₂O/SiO₂ = 44.9, Na/SiO₂ = 0.18, HMI/SiO₂ = 0.35. The synthesis mixture was stirred for 30 min at RT and then loaded into a Teflon-lined Parr reactor (300 cm³). Hydrothermal synthesis was carried out at 443 K for 40 h upon continuous stirring. The product, MCM-22 precursor (MCM-22P), was recovered by filtration, washed with distilled water, and dried at 383 K.

The MCM-56 was synthesized according to the method proposed by Fung et al. [14] with the synthesis gel composed of: SiO₂/Al₂O₃ = 23, OH/SiO₂ = 0.21, H₂O/SiO₂ = 20, Na/SiO₂ = 0.21, HMI/SiO₂ = 0.35. The resulting synthesis gel was stirred for 30 min at RT. Hydrothermal synthesis was carried out in a Teflon-lined Parr reactor at 416 K for 48 h upon continuous stirring. The resulting catalyst (MCM-56) was filtered off, washed with distilled water and dried at 383 K.

2.2. The modification of layered MWW zeolites

The zeolites obtained, MCM-22 and MCM-56, were modified in two steps. The first step of modification was swelling with surfactant hexadecyltrimethyl-ammonium chloride (CTMA-Cl) and tetrapropylammonium hydroxide (TPA-OH). The next step of modification

was pillaring with tetraethylorthosilicate (TEOS) and mixture of niobium source (niobium ethoxide) and silica (TEOS) as a new pillaring agent. We used two different procedures described by Roth (MCM-56 and MCM-22 before swelling were dried) [11] and Zhang (swelling was performed on wet catalysts) [12].

According the Roth's [11] procedure the MWW dried zeolites were mixed with cetyltrimethylammonium chloride (CTMACl, 25 wt%) (Aldrich) and tetrapropylammonium hydroxide (TPAOH, 40%) (Merck) at a relative weight ratio of 1:4.6:1.16. The mixture was continuously stirred at 363 K for 24 h. The resulting swollen material was filtered and washed with a small amount of distilled water and dried at 335 K overnight. The next step was pillaring of dried swollen MWW zeolites. Tetraethylorthosilicate (TEOS) (Aldrich) was added as a pillaring agent to the swollen MWW zeolite at a relative zeolite to TEOS weight ratio of 1:40. The mixture was stirred and heated under reflux at 368 K overnight. The solid was isolated by centrifugation, hydrolyzed in the centrifugation tube by adding 10–20 g of water and stirring overnight. It was then centrifuged and dried at 333 K overnight. Final calcination was carried out at 813 K for 5 h. To obtain NbMCM-36 zeolite, the pillaring procedures were modified by using a mixture of niobium source (niobium ethoxide) and silica (TEOS) as pillaring agents. The ratio of reagents was: MWW zeolite: TEOS: niobium ethoxide = 1:5:0.19.

The second method of modification of MWW zeolites was the Zhang's procedure [12]. The wet MWW zeolites (~25% of solid) were mixed with cetyltrimethylammonium chloride (CTMACl, 25 wt%) (Aldrich) and tetrapropylammonium hydroxide (TPAOH, 20%) (Merck) at a relative weight ratio of 1:4:1.2. The mixture was continuously stirred at 353 K for 72 h. The resulting swollen material was filtered and washed with a small amount of distilled water and dried at 335 K overnight. The next step was pillaring of dried swollen MWW zeolites. Tetraethylorthosilicate (TEOS) (Aldrich) was added as a pillaring agent to the swollen MWW zeolite at a relative zeolite to TEOS weight ratio of 1:5. The mixture was stirred and heated

under reflux at 353 K overnight. The solid was isolated by centrifugation and dried at 333 K overnight. Final calcination was carried out at 813 K for 5 h. To obtain NbMCM-36 zeolite, the pillaring procedures were modified by using a mixture of niobium source (niobium ethoxide) and silica (TEOS) as pillaring agents. The ratio of the reagents was: MWW zeolite: TEOS: niobium ethoxide = 1:5:0.19.

2.3. Techniques and conditions of samples characterization

N₂ adsorption/desorption isotherms were obtained using a Quantachrome Instruments Autosorb IQ2 at 77K. Before measurements the materials were outgassed under vacuum at 573 K. The surface area was calculated by the BET method. The volume of total pore volume was determined from BJH, whereas the micropore surface area and micropore volume were determined by the t-plot method. XRD patterns were obtained at r.t. on a Bruker AXS D8 Advance apparatus using CuK α radiation ($\lambda = 0.154$ nm), with a step of 0.05° in the wide-angle range. UV–Vis spectra were recorded using a Varian-Cary 300 Scan UV–Visible Spectrophotometer. Catalysts dried overnight at 373 K were put into the cell equipped with a quartz window. The spectra were recorded in the range between 190 - 800 nm. Spectralon was used as a reference sample. The content of metals in the catalysts was determined using an Spectrometer ICP-MS NexION 300d. Before the quantifications, the catalysts were mineralized using microwave acid digestion system (CEM Corporation USA Mars 5).

X-ray photoelectron measurements were acquired on an Ultra High Vacuum (UHV) System (Specs, Germany) working with a monochromatic microfocused Al K α X-ray source (1486.6 eV). Binding energies were referenced to the Si 2p peak at 103.4 eV.

Infrared spectra combined with pyridine adsorption were recorded using a Bruker Vector 22 FTIR spectrometer with an *in situ* vacuum cell. Before measurement, the solids were formed into thin wafers and placed inside the cell. The samples were then evacuated before pyridine adsorption at 623 K for 2 h. After this step, pyridine was admitted at 423 K. After

saturation with pyridine, the solids were degassed at 423 K, 473 K, 523 K and 573 K in vacuum for 30 min at each temperature. The spectrum without adsorbed pyridine (after sample activation at 673 K for 2 h) was subtracted from all recorded spectra. The numbers of Lewis and Brønsted acidic sites were calculated assuming the extinction coefficient ϵ for the band at $1447\text{ cm}^{-1} = 0.165\text{ cm}^2\mu\text{mol}^{-1}$ (Lewis acid sites) and for the band at $1545\text{ cm}^{-1} = 0.044\text{ cm}^2\mu\text{mol}^{-1}$ (Brønsted acidic sites) [15].

2.4. Test reactions

Cyclization and dehydration of 2,5-hexanedione (2,5-HDN)

The catalysts were tested for 2,5-hexanedione (2,5-HDN) dehydration and cyclization as the test reactions. A tubular, down-flow reactor (\varnothing 8 mm; length 180 mm) was used for the 2,5-HDN dehydration and cyclization reaction that was carried out at atmospheric pressure, using nitrogen as the carrier gas. The catalyst powder was pressed, crushed and sieved to the fraction of $0.5 < \varnothing < 1.0$ mm. A total of 0.05 g of this fraction was put into the reactor. The catalyst was first activated for 2 h at 623 K (heating rate 15 K min^{-1}) under nitrogen flow ($40\text{ cm}^3\text{ min}^{-1}$). Subsequently, a 0.5 cm^3 of 2,5-HDN (Fluka, GC grade) was passed continuously through the catalyst at 623 K. The substrate was delivered with a pump system (KD Scientific) and vaporized before being passed through the catalyst with the flow of nitrogen carrier gas ($40\text{ cm}^3\text{ min}^{-1}$). The reaction products were collected for 30 min downstream of the reactor in a cold trap (liquid nitrogen and 2-propanol) and analyzed by gas chromatography (SRI 310 C, MXT-1 column 30 m, temperature of column 373 K) with a TCD detector. Helium was applied as a carrier gas.

Liquid phase oxidation of cyclohexene with H_2O_2

The reaction was performed at 313 K in the liquid-phase, using acetonitrile as a solvent. The catalytic reaction between cyclohexene and hydrogen peroxide was carried out in and a glass reactor using the EasyMax Work Station equipped with a magnetic stirrer and a

thermocouple. A portion of 0.04 g of calcined catalyst was placed into the flask, and the solvent was added. After stirring of the mixture of solvent and the catalyst for 10 min at 313 K, cyclohexene (2 mmol) was added, followed by the dropwise addition of ~35% hydrogen peroxide (2 mmol). Samples (1 μ l) were withdrawn at regular time intervals and analyzed by a gas chromatograph of a SRI 310 chromatograph equipped with a capillary column DB-1 attached to a FID detector under nitrogen as a carrier gas. The catalysts were examined in the second run, i.e. after 30 h of the reaction and separation from the mixture by gyration. The catalyst was regenerated before the second reaction by calcination at 673 K for 4 h.

Degradation of methylene blue

The discoloration of methylene blue (MB) was carried out at room temperature. In a typical reaction, 0.1 g of catalyst was dispersed in 5 mL of hydrogen peroxide (30%). Next, 95 mL of MB solution (40 mg L⁻¹ or 80 mg L⁻¹) was added. In order to avoid photocatalytic degradation of methylene blue, the reactions were performed in the dark chamber. The dye discoloration was monitored using UV–vis spectroscopy (Varian, Cary 300 UV–vis spectrophotometer). For this purpose, after the proper time, 4 mL of the reaction mixture was removed, and the catalyst was separated from the solution by filtration through a 0.2 μ m Millipore filter. The efficiency of methylene blue removal was calculated using the following equation (Eq. (1))

$$\text{Efficiency of MB discoloration} = \frac{C_0 - C}{C_0} \times 100\% = \frac{A_0 - A}{A_0} \times 100\%$$

where A_0 is the absorbance of the initial MB solution, C_0 is the initial concentration of MB, A is the absorbance of the MB solution after a given time of the reaction, and C is the concentration of MB after a given time of the reaction; the absorbance was measured at 664 nm. For the sorption capacity measurements water was used instead of hydrogen peroxide.

3. Results and discussion

In MCM-36 materials obtained by modification of layered MCM-22 zeolite, the swelling and pillaring effect was better when the modifications were performed on dried catalyst according to the Roth's procedure. The surface area increased from 440 m²/g (MCM-22) to 763 m²/g (MCM-36_M22). In disordered MCM-56 zeolites more effective pillaring was achieved using the Zhang's procedure, the surface area increased from 408 m²/g (MCM-56) to 768 m²/g (MCM-36_M56). These results allowed us to select the most effective method to obtain NbMCM-36 zeolite, depending on the applied MWW zeolites (layered MCM-22 or disordered MCM-56).

3.1. Texture/structure characterization

Fig.1 presents X-ray diffraction patterns of the prepared zeolites: MWW precursors before calcination, which were used for further modification to obtain different MCM-36 zeolites and synthesized MCM-36 zeolites obtained by swelling and pillaring of different MWW precursors (layered MCM-22P and disordered MCM-56). There are two groups of materials obtained by pillaring with standard silica source (MCM-36_M22 and MCM-36_M56) and with niobosilicate used as a new pillaring agent (NbMCM-36_M22, NbMCM36_M56). In the symbols of MCM-36 materials, the starting zeolites are indicated after underscore (M22 stands for MCM-22, M56 means MCM-56). All prepared zeolites presented well-defined crystal structures. The use of niobosilicate as a pillaring agent gave a new type of MCM-36 zeolite. The XRD patterns of both, NbMCM-36 zeolites (obtained from layered MCM-22 and disordered MCM-56), show peaks typical of MWW structure. Moreover, no metal oxide phase was detected. Crystalline niobium(V) oxide should give the main XRD peaks at 2 theta of ca. 22.6, 28.3 and 36.6°. The absence of these peaks can be caused by good dispersion of Nb₂O₅, its amorphous state or substitution of Nb into the silica pillars of zeolites.

The N₂ adsorption-desorption isotherms are presented in Fig 2. The isotherms of the precursors, MCM-22 and MCM-56 were the same as presented by Zhang [12] for the same

materials. The first was typical of microporous materials (Fig. 2a), whereas the second (Fig. 2b) was characteristic of samples containing both, micro and meso/macropores. The isotherms of MCM-36_M56 (Fig. 2d) and NbMCM-36_M56 (Fig. 2f) were of type IV with a characteristic hysteresis loop starting at $p/p_0 \sim 0.4$. These results evidenced the formation of mesopores by pillaring with both silica and niobiosilicate. In the isotherms of both MCM-36 zeolites prepared by modification of layered MCM-22 the hysteresis loop was very small (Fig. 2c, e). The prepared zeolites show surface area and pore volume (Table 1) typical of MWW materials. A significant increase in BET surface of both MCM-36 and niobium containing zeolites in comparison with that of the starting materials (MCM-22 and MCM-56) evidenced that the modification was successful. Moreover, an increase in V_{total} and V_{meso} of pillared MCM-36 materials in comparison to those of MCM-22 and MCM-56 can be noted, which is a consequence of mesopores formation by pillaring. On the other hand, the V_{micro} values of pillared samples are lower than that of pristine MCM-22, probably due to the obstacle of inter-layer micropores by the pillars. The external surface area was estimated by t-plot. For MCM-36_M22 and MCM-36_M56 it was higher than for niobium containing zeolites.

3.2 State of niobium

The state of niobium present in modified zeolites was characterized by XPS and UV-vis spectroscopies. The UV-vis spectra of both niobium containing zeolites (Fig. 3A) are characterized by one symmetric band with the maximum intensity at ca. 220 nm, which was identified as corresponding to charge transfer in tetrahedrally coordinated niobium species located in the mesoporous silica framework. [16, 17]. The absorption band characteristic of octahedrally coordinated niobium species typical of bulk Nb_2O_5 at ca. 330 nm was not detected in the spectra of both NbMCM-36_M22 and NbMCM-36_M56. Thus, the UV-vis spectra confirmed the XRD results. For further investigation of niobium state and location in the zeolites the XPS spectroscopy was applied. This method analyzed the surface niobium species.

The results obtained for the prepared samples as well as for bulk niobium(V) oxide are shown in Table 2.

In both niobium containing zeolites, only niobium at +5 oxidation state was detected. The binding energies obtained for both NbMCM-36 zeolites are higher than those detected for bulk niobium oxide. The increase in the binding energies can be attributed to different surroundings of niobium species (Si-O-Nb) in the prepared MWW zeolites than in bulk niobium (V) oxide. The XPS results were used in the calculation of catalyst surface composition (Table 2). It can be noticed that the modification procedures (swelling and pillaring) caused slight changes in Si/Al ratio on the zeolite surface in the obtained MCM-36, except for the material (MCM-36_M22) prepared from the layered MCM-22 zeolite. There are also visible differences in the concentration of surface niobium incorporation by pillaring of layered MCM-22 and disordered MCM-56 zeolites. The material prepared from MCM-56 contains ca. 1.6 times more niobium species on the surface. Interestingly, the amount of niobium analyzed in the bulk material (ICP result-Table 2) was almost the same for both kinds of zeolites. Thus, disordered MCM-56 much more favors localization of Nb species on the surface than ordered MCM-22.

3.3. Acidity measurements

For identification of the type of acidic centers present on the zeolite surface, the infrared spectroscopy combined with the adsorption of pyridine as a probe molecule was applied. According to literature, after interaction of pyridine with Lewis acid sites (LAS) the characteristic bands at ~ 1450 and 1610 cm^{-1} appear [18, 19]. The intensity of the first band gives the information about the number of LAS, whereas the position of the second is related to the strength of LAS [18, 20]. Interaction of pyridine with Brønsted acid sites (BAS) is manifested by the infrared bands at ca 1550 cm^{-1} and two other ones at $1620\text{-}1640\text{ cm}^{-1}$. [20]. Pyridine can also interact with hydroxyl groups present on the surface of catalysts, forming

hydrogen bonds, giving rise to the bands at ca 1596 and 1445 cm^{-1} . The band at ca. 1490 cm^{-1} is characteristic of pyridine adsorbed on both LAS and BAS.

Fig. 4 presents the spectra (normalized to 10 mg of zeolite) of all the zeolites used. The spectra were recorded after pyridine adsorption at 423 K followed by evacuation for 0.5 h at 473 K. For all MWW zeolites, the bands characteristic of the interaction of the probe molecule with Lewis (1455 cm^{-1}) and Brønsted (1544 cm^{-1}) acid sites are well visible. For all samples the band assigned to pyridine adsorbed on both LAS and BAS (at ca 1490 cm^{-1}) dominates. Moreover, in the spectra of niobium containing samples two new bands at ca 1448 cm^{-1} and 1612 cm^{-1} are observed. These bands appeared after the interaction of pyridine with Lewis acid centers coming from niobium species. This result proves that pillaring of MWW zeolites with niobiosilicate resulted in generation of new active centers. Introduction of niobium into zeolites not only generated new LAS but also increased the number of BAS as shown in Table 3. Interestingly, the number of BAS in MCM-36 prepared without niobium source was much higher if MCM-56 was used as the starting zeolite. The strength of acid centers can be determined on the basis of the intensity drop of IR bands after evacuation of adsorbed pyridine with increasing temperature. Figs. S1-SD and S2-SD reveal the results of such evacuation for MCM-36 zeolites obtained by pillaring layered MCM-22 and disordered MCM-56 zeolites with silica and niobiosilicate. The acidic centers (BAS and LAS) characterized by the bands of pyridine chemisorbed (IR bands at 1544, 1622, 1637 cm^{-1} – BAS and 1455 cm^{-1} – LAS) coming from the starting zeolite structure (MCM-22 and MCM-56) are strong enough to chemisorb pyridine even after evacuation at 573 K. The decrease in the number of BAS occupied by pyridine after evacuation at 573 K (Table 3) decreased maximum of 27 % for NbMCM-36_M22 and only ~4 % for NbMCM-36_M56 in comparison with the number of BAS with chemisorbed pyridine after evacuation at 473 K. As shown in Figs. S1-SD and S2-SD the LAS generated by niobium introduction are not too strong and the bands characteristic of pyridine chemisorbed

on these centers (1448 and 1612 cm^{-1}) significantly decreased with increasing evacuation temperature. The difference in the behavior of BAS in MCM-36_M22 and MCM-36_M56 comes from the different Si/Al ratio (15 for the first and 12 for the second sample). The higher amount of Al in MCM-36_M56 results in the higher amount of BAS. The results shown in Table 3 indicate that all BAS in MCM-36_22 are strong enough to keep pyridine chemisorbed after evacuation at increasing temperature, whereas in the case of a higher amount of BAS in MCM-36_M56, a part of acidic centers is weaker and a part of pyridine desorbs after evacuation at increasing temperature. The strength of BAS was modified by the presence of Nb (the source of LAS). The higher amount of Nb in NbMCM-36_M56 caused the increase of BAS strength and therefore it was the lower drop of adsorbed pyridine upon temperature evacuation.

3.4. Cyclization and dehydration of 2,5-hexanodione (2,5-HDN)

The catalytic activity and acid/base properties of synthesized zeolites were tested in 2,5-hexanodione (2,5-HDN) transformation. This kind of reaction is often used as test reaction. In the presence of acid centers, 2,5-dimethylfuran (DMF) as a main product is formed, whereas the presence of basic centers is needed for formation of 3-methyl-2-cyclopentenone (MCP) [21, 22]. If acidic centers dominate on the surface of the catalyst, the selectivity ratio $\text{MCP}/\text{DMF} < 1$. The ratio $\text{MCP}/\text{DMF} > 1$ indicates that basicity is dominant. When $\text{MCP}/\text{DMF} \sim 1$, the tested catalyst has both acidic and basic character.

The results of cyclization and dehydration of 2,5-hexadione reaction performed over all prepared MCM-36 zeolite are collected in Table 4. All tested zeolites show very high conversion and high selectivity to DMF, which is formed in the presence of acidic centers. Modification of both layered and disordered zeolites by pillaring with niobiosilicate causes a decrease in the conversion of 2,5-HDN, which is especially visible for NbMCM-36_M56. The difference between activity of the MCM-36 zeolites prepared from MCM-22 and MCM-56, presented in Table 4, is not related to the number of BAS estimated from pyridine adsorption

but it should be correlated with structure/texture properties. Both MCM-36_M56 and NbMCM-36_M56 samples based on disordered MCM-56 are less active than those prepared from MCM-22. The disordering of zeolite structure decreases the effectiveness of cyclization process.

3.5. Liquid phase oxidation of cyclohexene with H₂O₂

To evaluate the catalytic activity of MWW zeolites, the prepared catalysts were tested in liquid phase oxidation of cyclohexene with hydrogen peroxide. The reaction was carried out at 313 K for 30 h in the presence of acetonitrile as a solvent. Fig. 5. presents the cyclohexene conversion *versus* the reaction time over both niobium containing zeolites and the same data for the reaction which was performed without catalysts (blank test). Cyclohexene oxidation with hydrogen peroxide performed in the absence of catalyst was negligible (2% of cyclohexene conversion). Application of niobium containing catalysts significantly increased the reaction rate leading to 50% (NbMCM-36_M56) and 44% (NbMCM-36_M22) of cyclohexene conversion after 30 h of the reaction. The high activity of niobium containing mesoporous silica in this reaction is well-known from literature [23-25] and can be explained by the ability of niobium to activate hydrogen peroxide [26]. This test reaction carried out over the catalysts prepared within this work confirmed the localization of niobium in niobiosilicate pillars, not in the zeolite framework, because the zeolites containing niobium in the skeleton did not show significant activity in this reaction [27]. The crucial role in catalytic oxidation of organic compounds like cyclohexene with hydrogen peroxide is played by chemisorption of H₂O₂, leading to the formation of peroxy or superoxy species. Metal peroxy or superoxy species can be detected by UV-vis measurements. To confirm the interaction of Nb containing zeolites with H₂O₂, the UV-vis spectra after treatment of the catalysts with hydrogen peroxide were performed (Fig. 3B). Both zeolites treated with H₂O₂ showed an increase in the adsorption

intensity in the range 300-400 nm, assigned to charge transfer from O_2^- (superoxo species) to niobium. [26, 28]

The cyclohexene oxidation reaction allows examination of participation of different active centers (Nb species- epoxide formation and acidic centers -diol generation) in the oxidation process. A few reaction pathways have been proposed in literature for the oxidation of cyclohexene with hydrogen peroxide [24], [25], [29]. Some of them are presented in Fig. 6. The formation of epoxide as a product of cyclohexene oxidation requires the presence of redox centers on the catalysts surface. Diols are formed in the next step of the reaction from epoxide, if the catalysts has strong acid centers (Fig. 6 route 2). This reaction pathway was observed for both tested niobium containing MWW zeolites. Fig. 7 displays the activity and selectivity of NbMCM-36_M22 and NbMCM-36_M56 zeolites after 5, 10 and 30 h of the reaction. After 5 hours of the reaction both catalysts ensured similar conversions (~20%) however different selectivities. For NbMCM-36_M56 the main product of the reaction was epoxide. It is worth pointing out that according to XPS analysis, this catalyst has a higher niobium concentration (Si/Nb=31). Different selectivity was observed for NbMCM-36_M22 (Si/Nb=49) in whose presence diol was the dominant product. After the next 5 hours of the reaction (10 h total) for both tested zeolites, the selectivity to epoxide increased, whereas after the following 15 h of the reaction (total 30 h) again the selectivity to diol dominated. Such volcanic changes in selectivity characterize bifunctional catalysts, in this work the catalysts containing the acidic centers for epoxide ring opening and the centers for activation of hydrogen peroxide towards formation of species active in epoxide formation. The reusability of catalysts is of great importance, especially when the reaction is performed in liquid phase in which leaching of active phase can occur. To check the stability of the catalysts, the zeolites were heated for 4 h at 673 K (the same conditions like before the first reaction) after the first reaction and used again at the same reagents ratio. The results for both niobium containing zeolites are presented in Fig. 8. Both

NbMCM-36 zeolites showed the same behavior. The activity of both tested zeolites increased in the second run. This effect was especially visible for NbMCM-36_M56, in whose presence the conversion of cyclohexene increased by about 10 %. Most probably the catalyst became activated during the heating after the first run because of the presence of non-reacted H₂O₂. It is known [26] that heating of niobium species in contact with H₂O₂ leads to the formation of reactive oxygen (superoxo/peroxo). What is important the materials used did not lose activity, the active phase was not leached.

3.6. Degradation of methylene blue

Oxidative properties of reactive oxygen species formed in the interaction with hydrogen peroxide on the niobium containing zeolites were evaluated by discoloration of methylene blue (MB). This reaction was performed at room temperature. At first the catalyst was dispersed in hydrogen peroxide, then methylene blue solution was added. In order to avoid photocatalytic degradation of methylene blue, the reactions were performed in the dark chamber. The dye discoloration was monitored by UV-vis spectrometer. The analysis was made after 15, 30 and 60 min of the reaction. The efficiency of discoloration of methylene blue is a result of two processes, adsorption (measured by experiments in water solution) and catalytic oxidation/degradation. To check the effect of the zeolites porosity on MB adsorption, we performed the reaction with pure MCM-36 zeolites obtained by pillaring layered and disordered MWW zeolites, without niobium. A solution with lower concentration of methylene blue (40 mg/L) was used. After the first 15 min of the reaction, 97 % of MB discoloration was observed for both tested zeolites and adsorption was the dominant process.

Fig. 9 shows the results of methylene blue discoloration performed on niobium containing zeolites. Because of the very high adsorption capacity detected in silica MWW zeolites with 40 mg/L of MB, in the experiment with NbMWW materials a higher concentration of MB was used (80 mg/L). After the first 15 min of the reaction ~60% of MB discoloration was observed

in the presence of both tested zeolites. Full discoloration of methylene blue was observed after 60 min of the reaction. Both niobium containing zeolites showed high activity in the discoloration of methylene blue, however their behavior was different. In the presence of NbMCM-36_M56 the reaction goes with degradation as a dominant process, whereas for the reaction with NbMCM-36_M22 the adsorption is the dominant one. Two reasons for the above mentioned behavior can be considered. One is the texture of both materials. The shape of hysteresis loop in N₂ adsorption/desorption isotherms (Fig. 2 f) indicates partial blockage of nitrogen desorption from micropores. This effect is more pronounced for NbMCM-36_M56. Therefore, adsorption of the dye is much easier in NbMCM-36_M22 structure, containing the lowest content of micropores, than in NbMCM-36_M56 one which contains more micropores (Table 1). Another explanation of this effect can be the different concentration of surface niobium species in both zeolites. According to literature data, hydroxyl radicals play a crucial role in this reaction [30]. Hydroxyl radicals can be formed by the interaction of H₂O₂ with hydroperoxo species (HO₂⁻). The interaction of the acidic surface hydroxyls with hydrogen peroxide give rise to formation of hydroperoxo species [28]. The role of niobium is to trap superoxo (O₂⁻) and peroxy (O₂²⁻) species on the surface, leading to production of the hydroxyl radicals. On the basis of the literature data mentioned above, it can be suggested that a higher concentration of surface niobium in the sample NbMCM-36_M56 (Si/Nb=31) gives higher concentration of hydroxyl radicals and hence a domination of discoloration process.

4. Conclusions

All prepared zeolites show well-defined crystal structure typical of MWW zeolites. Both methods used for modification of layered MCM-22 and disordered MCM-56 provided MCM-36 zeolites, as proved by XRD and adsorption/desorption isotherms. The use of niobosilicate as a pillaring agent gave a new type of MCM-36 zeolite. Niobium was present in tetrahedral coordination in pillars not in zeolite framework, and no Nb₂O₅ crystal phase was detected. The

efficiency of niobium incorporation to NbMCM-36 was much higher when disordered MCM-56 zeolite was used as starting material.

Niobium introduced to pillars of MCM-36 generated new Lewis acid sites of medium strength as evidenced by pyridine adsorption/desorption experiments. These sites played also a role of activator for hydrogen peroxide used in cyclohexane oxidation, in which NbMCM-36 zeolites were active catalysts. The dual centers, strongly acidic in the zeolite framework and niobium species in niobosilicate pillars took part in the oxidation of cyclohexene and led to the sinusoidal changes in selectivity to epoxide and diol, during the reaction time. Both niobium containing zeolites were stable and successfully used in the second run.

The texture of both NbMCM-36_M22 and NbMCM-36_M56 determined the properties of adsorption vs discoloration of MB. Moreover, the content of niobium in pillars was important for the effectiveness of MB discoloration.

Acknowledgements

We are grateful to the National Science Center in Poland for the financial support (project no. 2014/15/B/ST5/00167). The authors appreciate Mr M. Trejda's contribution in the experimental work.

References

- [1] M. Trejda, A. Wojtaszek, A. Floch, R. Wojcieszak, E.M.Gaigneaux, M. Ziolk, Catal. Today 158 (2010) 170-177.
- [2] M. Trejda, A. Wojtaszek, R. Wojcieszak, E.M. Gaigneaux, M. Ziółek; Stud. Surf. Sci. Catal., 175 (C) (2010) 445-448.
- [3] A.M. Prakash, L.Kevan L, J. Am. Chem. Soc. 120 (1998) 13148-13155.
- [4] S. Dzwigaj, Y. Millot, C. Méthivier, M. Che, Micropor. Mesopor. Mat. 130 (2010) 162-166.

- [5] A. Corma, I. Llabrés, F.X. Xamena, C. Prestipino, M. Renz, S. Valencia, *J. Phys. Chem. C* 113 (2009) 11306-11315.
- [6] A. Wojtaszek, M. Ziolk, S. Dzwigaj, F. Tielens, *Chem. Phys. Lett.* 514 (2011) 70-73.
- [7] F. Tielens, T. Shishido, S. Dzwigaj, *J. Phys. Chem. C* 114 (2010) 3140-3147.
- [8] A. Wojtaszek-Gurdak, M. Ziolk, *RSC Advances* 5 (2015) 22326-22333.
- [9] D. Prasetyoko, Z. Ramli, S. Endud, H. Nur, *Mater. Chem. Phys.* 93 (2005) 443-449.
- [10] A. Feliczak-Guzik, M. Sprynskyy, I. Nowak, M. Jaroniec, B. Buszewski, *J. Colloid Interface Science*, 516 (2018) 379-383.
- [11] J. Roth, P. Chlubna, M. Kubu, D. Vitvarowa, *Catal. Today*. 204 (2013) 8-14.
- [12] Z. Zhang, W. Zhu, S. Zai, M. Jia, W. Zhang, Z. Wang, *J. Por. Mater.* 20 (2012) 531-538.
- [13] M.E. Leonowicz, J.A. Lawton, S.L. Lawton, M.K. Rubin *Science*, 264 (1994), p. 1910.
- [14] A. S. Fung, S. L. Lawton and J. Roth, US Patent 5,362,697, 1994.
- [15] B. Gil, B. Marszałek, A. Micek-Ilnicka, Z. Olejniczak, *Top. Catal.* 53 (2010) 1340-1348.
- [16] B. Kilos, A. Tuel, M. Ziolk, J-C. Volta, *Catal. Today*, 118 (2006) 416-424.
- [17] D. Blasco-Jimenez, I. Sobczak, M. Ziolk, A. J. Lopez-Peinado, R.M. Martin-Aranda, *Catal. Today*, 152 (2010) 119-125.
- [18] M. Ziolk, I. Nowak and J.C. Lavaley, *Catal. Lett.* 45 (1997) 259-265.
- [19] G. Busca, *Catal. Today* 41 (1998) 191-206.
- [20] S. Khabtou, T. Chevreau, J.C. Lavalley, *Microporous Mater.* 3 (1994) 133-148.
- [21] R.M. Dessau, *Zeolites* 10 (1990) 205-206.
- [22] J.J. Alcaraz, B.J. Arena, R.D. Gillespie and J.S. Holmgren. *Catal. Today*. 43 (1998) 89-99.

- [23] J. Xin, J. Suo, X. Zhang, Z. Zhang, *New J. Chem.* 24 (2000) 813-814.
- [24] M. Ziolek, I. Nowak, I. Sobczak, A. Lewandowska, P. Decyk, J. Kujawa, *Stud. Surf. Sci. Catal.* 129 (2000) 813-822.
- [25] M. Ziolek, I. Nowak, *Zeolites* 18 (1997) 356-360.
- [26] M. Ziolek, I. Sobczak, P. Decyk and L. Wolski, *Chem. Commun.* 37 (2013) 85-91.
- [27] M. Ziolek, P. Decyk, I. Sobczak, M. Trejda, J. Florek, W. Klimas, H. Golinska, A. Wojtaszek *Appl Catal Gen* 391 (2011) 194–204.
- [28] M. Ziolek, I. Sobczak, P. Decyk, K. Sobanska, P. Pietrzyk, Z. Sojka: *Appl. Catal. B: Environmental* 164 (2015) 288-296.
- [29] F. Figueras, H. Kochkar, *Catal. Lett.*, 59 (1999) 79-81.
- [30] L. Wolski, M. Ziolek *Applied Catalysis B: Environmental* 224 (2018) 634–647.